Carbohydrate Polymers 116 (2015) 189–199

Contents lists available at ScienceDirect

Carbohydrate Polymers

journal homepage: www.elsevier.com/locate/carbpol

Microfluidics assisted generation of innovative polysaccharide hydrogel microparticles

M. Marquis, J. Davy, B. Cathala, A. Fang, D. Renard*

INRA, UR1268 Biopolymères Interactions Assemblages, F-44300 Nantes, France

ARTICLE INFO

Article history:
Received 6 November 2013
Received in revised form 20 January 2014
Accepted 24 January 2014
Available online 2 February 2014

Keywords:
Microfluidics
Droplets
Diffusion self-assembly
Pectin
Alginate
Janus
Shape

ABSTRACT

Capillary flow-based approach such as microfluidic devices offer a number of advantages over conventional flow control technology because they ensure highly versatile geometry and can be used to produce monodisperse spherical and non-spherical polymeric microparticles. Based on the principle of a flow-focusing device to emulsify the coflow of aqueous solutions in an organic phase, we were able to produce the following innovative polysaccharide hydrogel microparticles:

- Janus hydrogel microparticles made of pectin–pectin (homo Janus) and pectin–alginate (hetero Janus) were produced. The efficiency of separation of the two hemispheres was investigated by confocal scanning laser microscopy (CSLM) of previously labelled biopolymers. The Janus structure was confirmed by subjecting each microparticle hemisphere to specific enzymatic degradation. As a proof of concept, free BSA or BSA grafted with dextran, were encapsulated in each hemisphere of the hetero Janus hydrogel microparticles. While BSA, free or grafted with dextran, was always confined in the alginate hemisphere, a fraction of BSA diffused from the pectin to the alginate hemisphere. Methoxy groups along the pectin chain will be responsible of the decrease of the number of attractive electrostatic interactions occurring between amino groups of BSA and carboxylic groups of pectin.
- Pectin hydrogel microparticles of complex shapes were successfully produced by combining on-chip the phenomenon of gelation and water diffusion induced self-assembly, using dimethyl carbonate as continuous phase, or by deformation of the pre-gelled droplets off-chip at a fluid–fluid interface. Sphere, oblate ellipsoid, torus or mushroom-type morphologies were thus obtained. Moreover, it was established that after crossing the interface during their collect, mushroom-type microparticles did not migrate in the calcium or DMC phase but stayed at the liquid–liquid interface.

These new and original hydrogel microparticles will open up opportunities for studying relationships between combined enzymatic hydrolysis and active release for Janus particles and relationships between shape and swelling behaviour for anisotropic pectin microparticles.

1. Introduction

During the past decade, multi-compartment (Stahler, Selb, & Candau, 1999) and anisotropic particles with complex architectures (Jiang et al., 2010), have received significant attention due to their novel morphologies and diverse potential applications (Du & O'Reilly, 2011). Janus particles have two distinguishable surface areas of equal size, which makes them suitable for applications in switchable display devices (Nisisako, Torii, Takahashi, & Takizawa, 2006), interface stabilizers (Walther, Hoffmann, & Mueller, 2008), self-motile micro-particles (Howse et al., 2007), smart nanomaterials such as biological sensors, nanomotors, antireflection coatings (Yoshida & Lahann, 2008) and anisotropic building blocks for complex structures (Glotzer & Solomon, 2007). The name Janus particles was initially given by Cho and Lee in 1985 with polymerization of asymmetric poly(styrene)/poly(methyl methacrylate) emulsion (Cho & Lee, 1985) and many methods of producing these anisotropic particles have been developed over the last two decades (Lahann, 2011; Rahman, Montagne, Fessi, & Elaissari, 2010; Zhang et al., 2009).

Non-spherical particles or particles with complex architectures are more desired due to their unique properties such as anisotropic responses to external force, large surface area, and building blocks for hierarchical superstructures formation. Shape-controlled microbeads find applications in several fields such as the components of new flow measurement and regularly sized beads in liquid crystal displays (Yin & Xia, 2001) or as model systems to mimic anistropic biological cells and synthesize materials with

* Corresponding author. Tel.: +33 2 40 67 50 52; fax: +33 2 40 67 50 25.
E-mail address: drenard@nantes.inra.fr (D. Renard).

0144-8617/$ – see front matter © 2014 Elsevier Ltd. All rights reserved.
http://dx.doi.org/10.1016/j.carbpol.2014.01.083

unique crystal structure (Zheng, Tice, & Ismagilov, 2004). For the biological and medical areas, shape-controlled biocompatible and biodegradable hydrogel microparticles can be applied to drug delivery systems (Dai, Wang, & Zhao, 2005; De Geest, Urbanski, Thorsen, Demeester, & De Smedt, 2005; Zhang, Lewis, & Chu, 2005), cell immobilization (Sugiura et al., 2005), and cell cultures and biosensing fibres (Jeong et al., 2004; Yamada, Sugaya, Naganuma, & Seki, 2012).

Janus particles are currently produced by templating methods (Boeker, He, Emrick, & Russell, 2007; Charnay et al., 2003; Cui & Kretzschmar, 2006; Petit, Manaud, Mingotaud, Ravaine, & Duguet, 2001), colloidal assembly (Cho et al., 2007; Manoharan, Elsesser, & Pine, 2003), particle lithography techniques (Snyder, Yake, Feick, & Velegol, 2005), glacing-angle deposition (Perro, Reculusa, Ravaine, Bourgeat-Lami, & Duguet, 2005), nanosphere lithography (Haynes & Van Duyne, 2001) and capillary fluid flow. Methods to prepare particles with complex architectures are limited. Conventional emulsion polymerization and suspension polymerization to generate shape-controlled non-spherical microparticles are unpractical, because the minimization of interfacial energy leads to the formation of a spherical shape during most syntheses (Berkland, Kim, & Pack, 2001; Carturan, Dal Toso, Boninsegna, & Dal Monte, 2004). In recent years, a number of reports have emerged to directly address this bottleneck with the development of manipulation of previously fabricated spherical particles into non-spherical geometries and ab initio synthesis of non-spherical particles (Champion, Katare, & Mitragotri, 2007). Manipulation techniques such as film stretching or self-assembly are generally simpler than ab initio synthesis methods but usually cannot produce as diverse a range of shapes. Champion et al. were able to produce over twenty different three dimensional shapes using spheres as small as 200 nm by stretching spherical polystyrene particles embedded in a polymeric film and liquefied with heat or solvent (Champion & Mitragotri, 2006). Synthesis methods for generating non-spherical particles make use of the capillary flow-based approach such as microfluidics, often in combination with lithography and photopolymerization (Lewis et al., 2010; Nisisako & Hatsuzawa, 2009; Zhao et al., 2009).

The capillary flow-based approach offers a number of advantages over conventional flow control technology since they ensure highly versatile geometry and can be used to produce monodisperse spherical and non-spherical polymeric microparticles with diameters ranging from several tens to several hundreds of microns and a diverse range of shapes (Dendukuri, Tsoi, Hatton, & Doyle, 2005; Liu, Ding, Liu, Chen, & Zhao, 2006; Nie, Xu, Seo, Lewis, & Kumacheva, 2005; Seo, Nie, Xu, Lewis, & Kumacheva, 2005; Xu et al., 2005; Zhang, Betz, Qadeer, Attinger, & Chen, 2010). In most of the previous works, Janus particles produced by microfluidics were obtained from the polymerization of organic monomers by fast UV illumination (Nie, Li, Seo, Xu, & Kumacheva, 2006; Nisisako et al., 2006). Several groups used microfluidic devices to produce non-spherical polymeric microparticles by first producing in the microchannels prepolymer microparticles with the desired shape and second using a UV-photopolymerization process to solidify microparticles (Nie et al., 2005; Seo et al., 2005). Xu et al. and Dendukuri et al. for instance formed liquid droplets with a microfluidic device, shaped the droplets in a microchannel and polymerized them to form solid particles of several non-spherical geometries (Dendukuri et al., 2005; Xu et al., 2005). Unfortunately, the UV-polymerization process is very hazardous to biological applications and UV-sensitive materials and all these strategies are limited to light-sensitive compounds.

Hydrogel-based microparticles, in contrast, are hydrophilic polymer networks with a high affinity for water. These microparticles have recently been used in tissue engineering, drug delivery and bionanotechnology (Chawla, Yu, Liao, & Guan, 2011; Peppas, Hilt, Khademhosseini, & Langer, 2006; Siracusa, Rocculi, Romani, & Dalla Rosa, 2008; Ulery, Nair, & Laurencin, 2011). In general, biopolymer particles with the appropriate properties for releasing or immobilizing the products of interest have been produced by solution-based batch methods (Bellich, Borgogna, Cok, & Cesaro, 2011; Liu et al., 2003; Poortinga, 2008) but also by microfluidic techniques that allow precise control of the fluid velocities and droplet volumes. Pectin and alginate are environmentally friendly since they are highly water soluble, biocompatible and biodegradable. One feature of these biopolymers is their high content of carboxylic groups that can be ionically cross-linked to achieve the formation of gels (Ouwerx, Velings, Mestdagh, & Axelos, 1998; Ralet, Bonnin, & Thibault, 2001; Zykwinska, Gaillard, Boiffard, Thibault, & Bonnin, 2009). In the last decade, versatile microfluidic technologies have emerged for the fabrication of biopolymer particles of controlled size, shape and composition (Dang & Joo, 2013; Hu et al., 2012; Liu et al., 2006; Rondeau & Cooper-White, 2008; Serra & Chang, 2008; Yamada et al., 2012; Yang et al., 2012; Zhang, Tumarkin, Sullan, Walker, & Kumacheva, 2007). However, Janus particles using two chemically distinct biopolymers has not yet been achieved and remains a challenge due to both diffusive intermixing and convective transport in the microchannels (Sarrazin, Bonometti, Prat, Gourdon, & Magnaudet, 2008). Moreover, in the development of anisotropic microparticles with complex shapes, the recent process called microfluidics diffusion-induced self-assembly (μfDISA), exploiting the properties of the dimethyl carbonate as continuous phase to control water uptake from droplets (Fang, Gaillard, & Douliez, 2011; Fang, Gosse, Gaillard, Zhao, & Davy, 2012), in order to control the shape and size of microparticles, has never been demonstrated on polysaccharides.

We first describe a microfluidic device for the generation of monodisperse homo and hetero Janus hydrogel microparticles using pectin–pectin and pectin–alginate hydrogels. As the polysaccharides used are completely miscible in a wide range of concentrations, the challenge in microfluidic design was to obtain a well-defined interface between the two biopolymer hemispheres in the homo and hetero Janus microparticles. Second, we demonstrate the ability to design pectin hydrogel microparticles with complex shapes by combining a strategy of biopolymer gelation and diffusion-induced self-assembly process using dimethyl carbonate, able to shrink and deform the pre-gelled droplets due to its water immiscibility and solubility. Pectin as source of renewable resources and $CaCl_2$ or $CaCO_3$ as source of calcium were used to form hydrogel microparticles and shape was controlled on-chip by solvent diffusion or off-chip by deformation of the pre-gelled droplets at a fluid–fluid interface.

2. Materials and methods

2.1. Materials for Janus microparticles production

Low-methoxyl citrus pectin (M_w = 169 250 g/mol, M_w/M_n = 2.03) was purchased from Cargill France SAS, and had a degree of esterification (DE) of 30% and contained 78.5% galacturonic acid. Alginate (M_w = 151 550 g/mol, M_w/M_n = 2.11), of medium viscosity, was obtained from FMC biopolymer (USA). Bovine serum albumin (BSA) was purchased from Sigma–Aldrich (lot n° 1379622). N-(3-dimethylaminopropyl)-N′-ethyl-carbodiimide hydrochloride (EDC) (Sigma–Aldrich, France) and N-hydroxysuccinimide (NHS) (Sigma–Aldrich) were used for covalent coupling of fluoresceinamine (FA) (Sigma–Aldrich, France) (λ_{exc} 485, λ_{em} 535 nm) and Bodipy TR cadaverine (Invitrogen, France) (λ_{exc} 588, λ_{em} 616 nm) to citrus pectin or alginate through activation of the polysaccharide carboxyl groups as described by Ogushi, Sakai and Kawakami (2007). Sodium alginate, sodium FA-alginate, citrus pectin, citrus

FA-pectin and citrus Bodipy-pectin were prepared at 2 wt% concentrations and dissolved in deionized water for 2 h. The pH value for both biopolymer solutions was then adjusted to around 7 with NaOH 1 M to obtain low viscosities and to minimize the onset of gelation due to the presence of acid compounds. Freeze-dried calcium carbonate ($CaCO_3$) powder (5 μm diameter particles) was dispersed in deionized water at 1 wt% concentration. Calcium carbonate and biopolymer solutions were then mixed at a 1:1 (v:v) ratio to give final concentrations of 0.5 wt% and 1 wt% for the calcium carbonate and biopolymer solutions, respectively. The oil phase was sunflower seed oil (Fluka) either mixed with Span 80 (Sigma–Aldrich) (1 wt%) or with Span 80 (1 wt%) and acetic acid (0.5 wt%).

Polygalacturonase type II (PGII) from *Aspergillus Niger* was purchased from Novozymes (Bagsvaerd, Denmark). Alginate lyase (AL) from *Sphingobacterium multivorum* was purchased from Sigma–Aldrich, France. Enzyme solutions of PGII and AL were prepared in deionized water at 3 wt% (w/w) and 0.25 wt% concentrations, respectively.

2.2. BSA encapsulation in hetero Janus microparticles

To visualize BSA encapsulated in each hemisphere of hetero Janus microparticles, grafting of FITC (Sigma–Aldrich, lot n° 1302813) or RITC-Dextran (Sigma–Aldrich, lot n° 041M5309V) to BSA was applied. BSA was dissolved in 100 mM sodium carbonate buffer pH 9.2 at $C = 0.0125$ wt% then 0.5 wt% of FITC or RITC-Dextran, previously dissolved in DMSO, was gently added to BSA solution under vigorous stirring. The mixture was left overnight at $T = 4\,^{\circ}C$ under stirring in the dark. Dialysis was performed using Spectra/Por© bags (cutoff 3500 Da) against distilled water during two days in order to remove free fluorescent markers. FITC-BSA and RITC-Dextran-BSA were then freeze-dried and stored in the dark before use.

2.3. Microfluidic device for Janus microparticles production

A microfluidic system, comprising a Flow Focusing Device (FFD) and a second inlet for the continuous phase, was prepared using poly(dimethylsiloxane) (PDMS) (RTV 615, Elecoproduit, France) and a soft lithography technique (Y.N. Xia, G.M. Whitesides, Annu. Rev. Mater. Sci. 28 (1998) 153). SU-8 (CTS, France) positive relief structures were produced on silicon wafers. PDMS polymer (in a mixture of 10:1 base polymer:curing agent) was cast from this mould, and access holes were punched on the PDMS layer. The PDMS layer (in a mixture of 10:1 base polymer:curing agent) was then placed in contact with a thin PDMS layer (in a mixture of 20:1 base polymer:curing agent) to generate the microchip. The cross-linker diffused as a result of the gradient from PDMS (10:1) to PDMS (20:1). The chip was then oven-treated at 70 °C for 24 h to strengthen the cross-linking. The microchannels were rectangular in shape with a uniform height of 120 μm and respective widths of 75 μm for the biopolymer phases, 150 μm for the oil phase, 100 μm for the restriction and 200 μm for the central channel as determined by profilometry.

2.4. Emulsion of aqueous solutions of biopolymer and preparation of Janus microparticles

Aqueous solutions of biopolymers with $CaCO_3$, a sunflower seed oil with surfactant (Span 80) and a sunflower seed oil with surfactant and acetic acid were supplied to the microchannels using digitally controlled syringe pumps (Harvard Apparatus PHD 2000, France) (Fig. 1). The biopolymer hydrogel microparticles generated by the microfluidic Flow Focusing Device were produced by internal gelation (Zhang et al., 2007). The droplets contained pectin and/or alginate and $CaCO_3$ as the crosslinking agent in an inactive form. The continuous phase (sunflower seed oil) contained acetic acid (0.5 wt%) which diffused into the droplets and triggered the

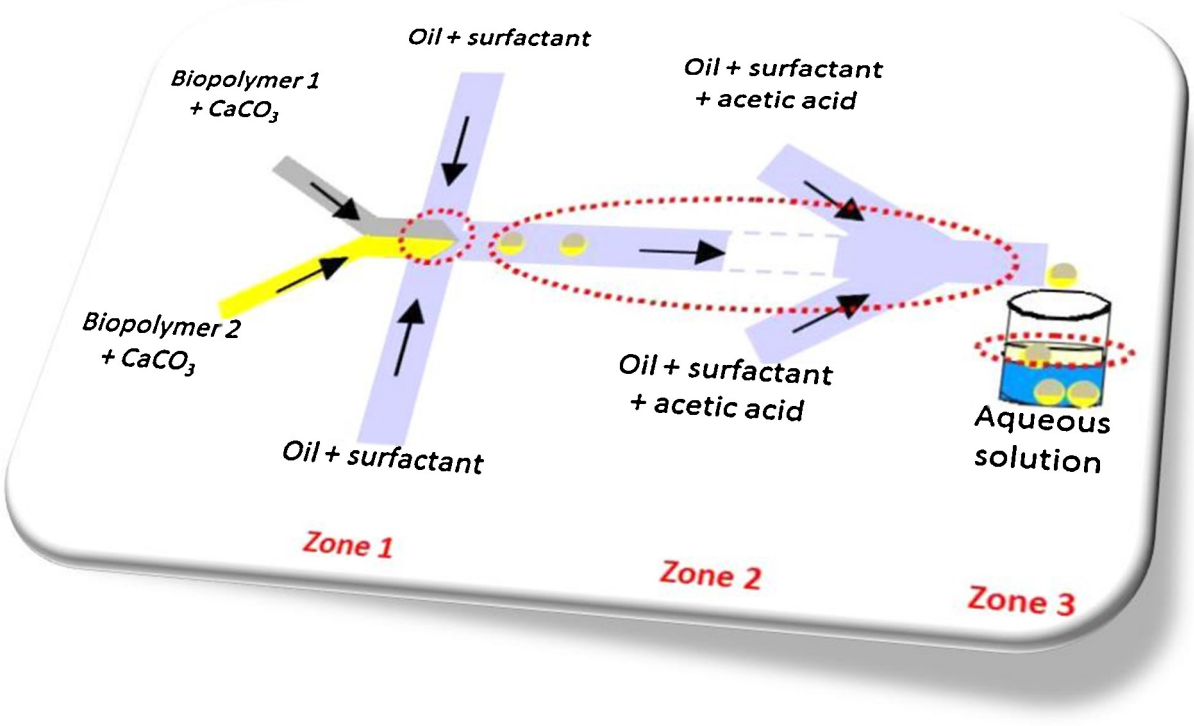

Fig. 1. Schematic representation of the microfluidic device for Janus droplet generation using a micro flow focusing device with inlets for the two biopolymers mixed with an inactive form of the crosslinking agent ($CaCO_3$) emulsified in oil (zone 1). Droplet gelation was induced by the diffusion of acetic acid from the oil phase to the droplets where the resulting pH decrease inside the droplets led to calcium bridging and thus to biopolymer gelation (zone 2). The pre-gelled droplets were collected off-chip in a $CaCl_2$ (1 wt%) solution bath (zone 3).

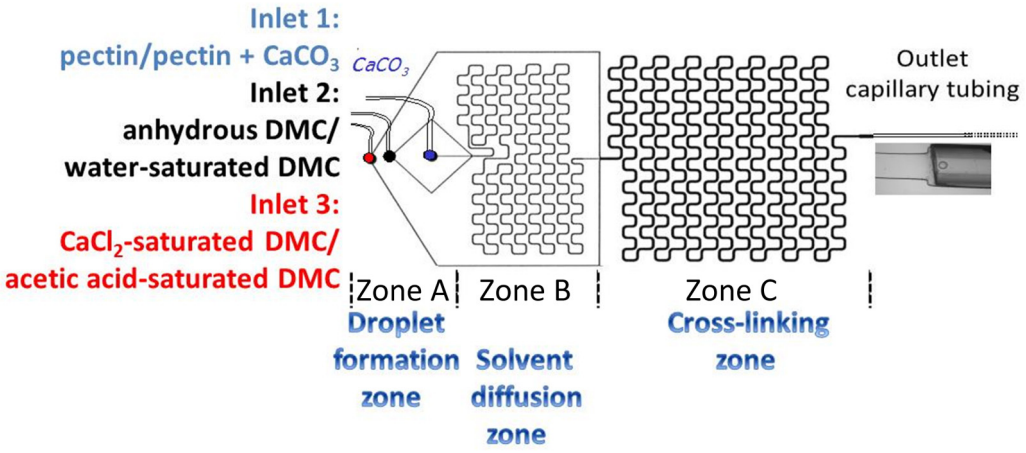

Fig. 2. Schematic of the microfluidic flow-focusing geometry used for pectin hydrogel microparticle formation; a pressure-driven flow controller was used for supplying the three liquids to the device: pectin or pectin + carbonate calcium ($CaCO_3$) (inlet 1), anhydrous or water-saturated dimethyl carbonate (DMC) (inlet 2) and DMC + calcium chloride ($CaCl_2$) or DMC + acetic acid (inlet 3). An outlet capillary tubing allowed the hydrogel microparticles to be collected in a $CaCl_2$ bath. Zone A: pectin microdroplet generation zone thanks to flow-focusing geometry. Zone B: solvent diffusion zone thanks to anhydrous dimethyl carbonate (DMC). Zone C: cross-linking zone thanks to calcium ions diffusion within pectin microdroplets.

release of Ca^{2+} ions, resulting in crosslinking of the polysaccharide chains and thus the formation of a biopolymer network. The hydrogel microparticles were collected in a bath of $CaCl_2$ (1 wt%) solution, gently washed in water then centrifuged (440 × *g*, 5 min) to remove the residual oil phase and $CaCl_2$.

2.5. Selective enzymatic hydrolysis of hetero Janus microparticles

The enzymatic hydrolyses were performed using either polygalacturonase type II (PGII) or alginate lyase (AL) and Bodipy-pectin/FA-Alginate microparticles as substrates. Reaction mixtures containing 28 μl of deionized water, 2 μl of microparticle solutions and 10 μl of PGII at 3 wt% or AL at 0.25 wt% concentrations were incubated at 40 °C for 25 min or at room temperature for 10 min, respectively. Enzymatic degradation of the microparticles, which depended on the enzyme used, was qualitatively evaluated using visualization by fluorescence coupled with phase contrast microscopy and by confocal microscopy.

2.6. Imaging of Janus hydrogel microparticles

Phase contrast and fluorescence microscopy images were captured with an Olympus IX51 inverse microscope (Olympus, France) equipped with phase contrast illumination, a standard green filter (Exciter filter (BP) 460–490 nm, Dichroic Mirror (DM) 500, Barrier Filter (BA) 520 nm), a standard red filter (BP 510–550 nm, DM 570 nm, BA 590 nm) and a digital camera (Sony, SCD-SX90). The size distributions of the microbeads were analyzed using the ImageJ freeware v1.35c.

Confocal microscopy images were captured using a Nikon Ti-E with C1si scanning laser confocal microscope (Nikon, France) and a Nikon Eclipse Ti inverse microscope (Nikon, France). FA and FITC emission fluorescence were recorded between 500 and 530 nm after excitation at 488 nm. Bodipy and RITC-Dextran emission fluorescence were recorded between 570 and 620 nm after excitation at 561 nm.

2.7. Microfluidic device for pectin hydrogel microparticles production

Microfluidic device was prepared using poly(dimethylsiloxane) (PDMS) (RTV 615, Elecoproduit, France) and a soft lithography technique as described previously for Janus microparticles production. The microchannels were rectangular in shape with a uniform height (*h*) of = 100 μm. The microsystem was made of three zones: a flow focusing Junction where droplets of pectin were formed (zone A), a first serpentine channel where droplets shrunk by solvent diffusion (zone B) and a second serpentine channel where cross-linking within pectin microdroplets took place through calcium bridging (zone C) (Fig. 2). The widths and lengths of serpentine channels in zones B and C were, respectively, of 200 μm and 52 cm and 450 μm and 98 cm.

2.8. Chemical and solutions for pectin hydrogel microparticles production

Pectin was solubilized in 50 mM MES buffer pH 6 at *T* = 40 °C or in deionised water at room temperature under magnetic stirring during 2 h then stored at *T* = 4 °C. The pectin solutions were degassed under vacuum and filtered through a 5 μm filter (PURADISC filter, FP 30 mm 5.0CN, Whatman). The pH value of pectin solutions prepared in deionised water was then adjusted to around 7 with NaOH 1 M. Anhydrous dimethyl carbonate 99% (DMC) (ref. D152927-1L), calcium chloride, carbonate calcium and acetic acid were purchased from Sigma–Aldrich (France). EDC and NHS were used for covalent coupling of FITC to citrus pectin through activation of the polysaccharide carboxyl groups, as described by Ogushi et al. (2007).

2.9. Preparation of pectin hydrogel microparticles

2.9.1. Emulsification and shrinkage of pectin microdroplets

Pectin microdroplets were achieved by emulsifying 5, 10 or 20 μg/μL aqueous solution of pectin in DMC as the continuous oil phase in the microfluidic devices. The aqueous liquid phase broke up in continuous oil phase to generate W/O emulsion microdroplets in zone A (Fig. 2). The two immiscible liquids were supplied to the microchannels using a Microfluidic Flow Control Systems, MFCS-4C-1000 (Fluigent, France) as a pressure-driven flow controller. The PDMS device was linked to the MFCS through polytetrafluoroethylene (PTFE) tube (0.3 mm i.d. × 0.76 mm o.d. and length, 350 mm) (Fisher Scientific, ref. 39240). The size of the microdroplets was controlled by varying the pressure of the two immiscible liquids. DMC with water content in the range of 0-saturation was used as the continuous phase allowing the

shrinkage in zone B by solvent diffusion. Water-saturated DMC was prepared by magnetic stirring DMC in the presence of a large quantity of water for at least 2 h. The bottom phase was used as water-saturated DMC. DMC with water content between 0 and saturation was prepared stoichiometrically mixing DMC with its water-saturated counterpart. Images of microdroplets formation and shrinkage were captured using an Olympus IX51 inverse microscope (Olympus, France) equipped with a digital camera (Hamamatsu C4742-95).

2.9.2. Pectin hydrogel microparticles formation

Pectin cross-linking occurred in zone C by internal or external gelation mode (Fig. 2). Internal gelation mode was induced by a pH decrease inside the microdroplets. The microdroplets contained pectin (0.5, 1 or 2 wt%) and $CaCO_3$ (0.25, 0.5 or 1 wt%) as the crosslinking agent in an inactive form. The continuous phase (DMC) was saturated by acetic acid aqueous solution (0.5 wt%) which diffused into the microdroplets and triggered the release of Ca^{2+} ions, resulting in the cross-linking of pectin chains and the formation of a network. External gelation mode was performed by the diffusion of a solubilized cross-linker from the continuous phase to the microdroplets. The continuous phase (DMC) was saturated by calcium chloride ($CaCl_2$) aqueous solution (0.9 wt%). Cross-linking was induced by rapid diffusion of calcium ions inside pectin microdroplets resulting in a network formation. In both cases, pectin hydrogel microparticles were collected in a bath of $CaCl_2$ (2 wt%) solution.

2.10. Imaging of pectin hydrogel microparticles

The microparticles collected off-chip were analyzed using an Olympus IX51 inverse microscope (Olympus, France) equipped with phase contrast and brightfield illuminations and a digital camera (Sony, XCD-SX90). Some hydrogel microparticles with non-spherical shapes were also observed using a Nikon Ti-E with C1si scanning laser confocal microscope (Nikon, France) and a Nikon Eclipse Ti inverse microscope (Nikon, France) after pectin labelling using fluoresceinamine isothiocyanate (FITC). FITC emission fluorescence was recorded between 500 and 530 nm after excitation at 488 nm.

For scanning electron microscopy (SEM), hydrogel microparticles were prepared by the supercritically-dried method known to retain most of the volume of the parent hydrogel and to present high surface areas (Robitzer, David, Rochas, Di Renzo, & Quignard, 2008). Liquid CO_2 and water are not directly miscible. As a consequence, in order to prepare the samples for supercritical drying, the hydrogel microparticles had to be dehydrated by immersion during 15 min in hydroalcoholic solutions of increasing ethanol concentration (10, 30, 50, 70, 90 and 100%) then in anhydrous ethanol and acetone. Acetone was later exchanged by liquid CO_2 in a Balzers Union CPD030 chamber, in which the samples were heated beyond the CO_2 critical point (20 °C, 50 bars) and outgassed by successive purges of the chamber to obtain the aerogel microparticles. The temperature and final pressure were then increased to 40 °C and more than 73.8 bars, respectively, to be in CO_2 supercritical conditions. Samples were finally stored in a dessicator containing anhydrous P_2O_5. Samples observations were made using a Jeol 6400F microscope operating at 3 kV after gold/palladium thin coating of the samples during 5 min mounted on double sided carbon grids. We first checked on bulk spherical gels ($D \sim 2$ cm, $C = 10$ μg/μL) that the supercritically-dried process did not impact the shape of the aerogel, only size changes occurred (a 40% reduction in size was noticed) (data not shown).

3. Results

3.1. Device optimization for the generation of Janus hydrogel microparticles

Although the microfluidics process used to obtain Janus particles takes advantage of laminar flow (Shepherd et al., 2006), it is important to note that diffusive intermixing may occur with miscible fluids in a two-phase stream before the droplets break up. In fact, the low Reynolds number in the channel before the junction ($R_e < 1$) indicates that non convective transport can occur across the two parallel streams. However, symmetric recirculation is induced inside the forming droplets by co-flowing of the external streams (Nisisako et al., 2006). Furthermore, the contact between droplet and channel walls increases the impact of convection and the occurrence of internal recirculation loops (Sarrazin et al., 2008). Thus the internal recirculation loop phenomenon can disappear when the contact with the wall and the internal droplet velocity are reduced. Finally, the droplet diameter needs to be less than 80% of the channel width in order to inhibit the exchange of material caused by internal circulation during co-flowing. In this context, the channel containing the two miscible phases of the biopolymers (FA-pectin and Bodipy-pectin or FA-alginate and Bodipy-pectin), the geometry of the flow focusing junction and the central channel were therefore adjusted so as to minimize diffusive intermixing (Fig. 2). The central channel was therefore short and large (depth: 100 μm, width: 200 μm and length: 22 mm) and without any zones of turbulence, such as a serpentine shape or the pressure variations commonly used to optimize mixing inside the droplets or coalescence (Tung, Li, & Yang, 2009; Um, Lee, Pyo, & Park, 2008). The outlet at the end of the PDMS microcircuit was therefore parallel to the central channel and without a swimming pool. Indeed, at the end of the central channel, gelation was incomplete and a swimming pool outlet would have resulted in high pressure variations. Pre-gelled microbeads would therefore be distorted and finally fuse by coalescence. Another critical zone in the microcircuit was the parallel outlet where diffusive intermixing phenomena were limited by using a polytetrafluoroethylene (PTFE) tube (0.3 mm i.d. × 0.76 mm o.d. and length: 20 cm) directly inserted in a PDMS short exit channel (depth: 100 μm, width: 400 μm and length: 5 mm). Internal gelation was obtained by using calcium carbonate and acidification (Zhang et al., 2010). Gelation beyond the FFD junction had to be delayed in order to limit cap-formation at the junction. Thus a second inlet of the continuous phase was added 2 mm away from the junction to delay diffusion of the acetic acid in the sunflower seed oil (Fig. 2). The flow rates for FA-pectin or FA-alginate, Bodipy-pectin and oil in each channel, were, respectively, 1, 1 and 18 μl min^{-1}. The resulting homo and hetero Janus microparticles had an average diameter of 92 μm.

3.2. Generation of homo and hetero Janus hydrogel microparticles

Fluorescently-labelled (Fluoresceinamine, FA and Bodipy Tr cadaverine, Bodipy) pectins were prepared in order to visualize the co-flowing aqueous stream and the production of fluorescent homo Janus particles. The fluorescence micrographs taken after gelation (Fig. 3a) showed fluorescently-labelled hemispheres within the droplets, composed of FA-labelled and Bodipy-labelled pectin. This process was highly reproducible. The hydrogel microparticles were then collected at the end of the microcircuit in an aqueous solution of $CaCl_2$ to ensure maximal cross-linking and to limit the coalescence of homo Janus microparticles. Initial observations by fluorescence microscopy, with the appropriate filters (results not shown), showed that FA-pectin and Bodipy-pectin were concentrated on opposite sides of the hemispheres. However, the interface

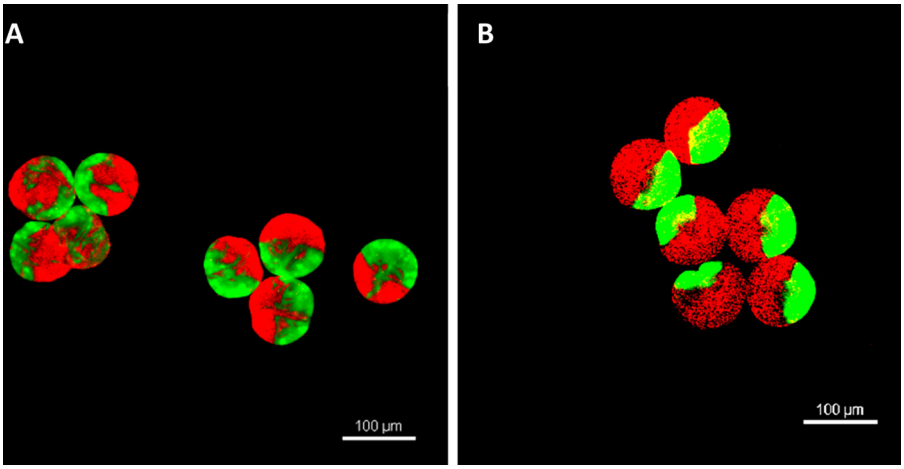

Fig. 3. Fluorescence confocal microscopy images for FA-pectin/Bodipy-pectin homo Janus (A) and FA-alginate/Bodipy-pectin hetero Janus (B) hydrogel microparticles. Fluoresceinamine (FA) and Bodipy excitations were set at 488 nm and 561 nm respectively while emission fluorescence was recorded between 500 and 530 nm (green) and between 570 and 620 nm (red). The flow rates of FA-pectin (or FA-alginate), Bodipy-pectin and oil in each channel were 1, 1 and 18 µl min^{-1}, respectively. Scale bars: 100 µm. (For interpretation of the references to colour in this figure legend, the reader is referred to the web version of this article.)

was not clearly defined, which suggested that some diffusive intermixing occurred (Fig. 3a).

Fluorescent FA-labelled alginate and Bodipy-labelled pectin microbeads were prepared under the same conditions as for homo Janus microbeads. The alginate/pectin microbeads also displayed two distinct hemispheres but the interface was well-defined, clearly indicating that only limited diffusive intermixing occurred (Fig. 3b). A specific interaction, hydrogen bonds between the methoxyl groups in pectin and the hydroxyl groups in the guluronic acids of alginate (Gohil, 2010), would lead to a decrease in long range molecular motions at the interface and therefore reduce the linear distance of diffusive intermixing, thus creating a better separation at the interface of hetero Janus microbeads (Fig. 3b) (Marquis, Renard, & Cathala, 2012).

3.3. Selective enzymatic hydrolysis of hetero Janus hydrogel microparticles

The feasibility of selective degradation was demonstrated and the Janus architecture confirmed by investigating the effect of specific enzymes against each of the polysaccharides presents in the hetero Janus microbeads. A polygalacturonase (PGII) from Aspergillus Niger was used to hydrolyse the backbone, especially the 1–4 linkages between adjacent α-D-GalA residues present in pectin (Bonnin et al., 2002). Alginate degradation was achieved by using an alginate lyase (AL) from *S. multivorum*, also known as alginase or alginate depolymerase. This enzyme catalyzes the hydrolysis of alginate by a β-elimination mechanism targeting the glycosidic 1 → 4 O-linkages between monomers (Thiang Yian, Preston, & Schiller, 2000). The enzymatic hydrolyses clearly revealed the degradation of the desired hemisphere in the microparticles (Fig. 4). Indeed, FA-alginate/Bodipy-pectin microparticles mixed with PGII showed a single green fluorescent hemisphere, implying total degradation of the pectin, after 25 min of incubation at 40 °C (Fig. 4a). The persistence of red fluorescence at the end of the experiment could be due to a progressive decrease of PGII activity due to the release of calcium ions from the pectin network. The presence of calcium salts (except for dibasic calcium phosphate and calcium tartrate), is known to inhibit PGII activity (Biggs, ElKholi, ElNeshawy, & Nickerson, 1997). On the other hand, hydrogel microparticles mixed with alginate lyase displayed a single red fluorescent hemisphere, which suggested the total degradation of alginate, after 10 min of incubation (Fig. 4b). Moreover, the presence of either PGII or AL did not affect the stability of the non-degraded hemispheres in the hetero Janus microparticles over time. These original results demonstrate the increased flexibility of hydrogel microparticles derived from polysaccharides and open up possibilities in controlled release, particularly the time-controlled release of two active compounds embedded in each of the microparticle hemispheres in response to specific enzymatic hydrolyses.

3.4. Encapsulation of BSA in hetero Janus hydrogel microparticles

As a proof of concept, free BSA or BSA grafted with dextran, were encapsulated in each hemisphere of the hetero Janus microparticles (Fig. 5). While BSA, free or grafted with dextran, was always confined in the alginate hemisphere (Fig. 5a and b), this was not the case when BSA was encapsulated in the pectin hemisphere (Fig. 5c and d). The diffusion of BSA from pectin to alginate hemisphere was confirmed in the yellow colour of the alginate compartment after colour superimposition of the confocal images (Fig. 5e and f). This result was found to be explained by the electrostatic interactions between carboxylic groups of polysaccharides and amino groups of BSA. In the case of pectin, methoxy groups present along the chain decrease the number of attractive electrostatic interactions between BSA and pectin, resulting in a diffusion of a fraction of BSA, free or grafted with dextran, from the pectin to the alginate hemisphere. Around 10% BSA diffusing from pectin to alginate hemisphere was estimated from fluorescence kinetics measurements (data not shown).

3.5. Device optimization for the generation of pectin hydrogel microparticles

Two alternative processes coupled to two modes of gelation were used to produce pectin hydrogel microparticles. One process involved a shrinkage step through solvent diffusion process before internal or external gelation took place, the other process allowed the production of pectin hydrogel microparticles by internal or external gelation without a preliminary shrinkage step. Contrary to the work of Rondeau and Cooper-White (2008) on alginate production by microfluidics where solvent diffusion and gelation simultaneously occurred, the pectin hydrogel microparticles formation in our study was followed either by only a change of size due to solvent diffusion process or by modifications both

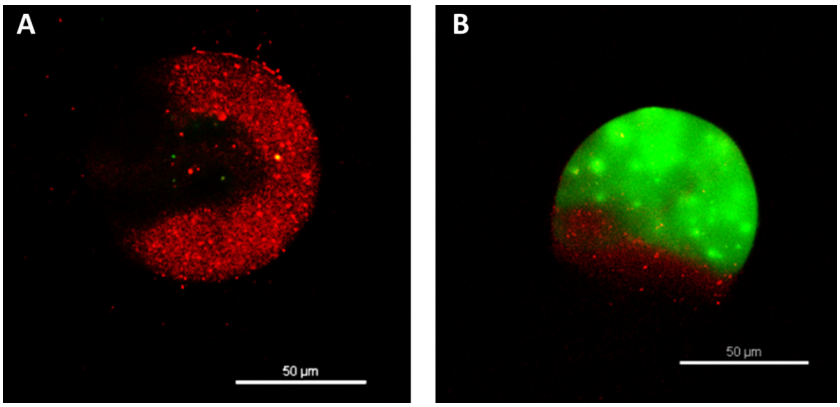

Fig. 4. Confocal scanning laser microscopy images of the enzymatic degradation of fluorescently labelled pectin–alginate hetero Janus hydrogel microparticles. (A) Enzymatic degradation of FA-alginate hemisphere by Alginate Lyase. (B) Enzymatic degradation of Bodipy-pectin hemisphere by Polygalacturonase II. Mixing conditions were: 28 µl deionized water, 2 µl of microparticle solution, 10 µl of enzyme solution. Scale bars: 50 µm.

in size and shape due to an elapsed time between solvent diffusion and gelation processes (Fig. 2). In addition, the properties of the dimethyl carbonate continuous phase towards water solubility allowed the solvent diffusion to proceed (when DMC was anhydrous) or not (when DMC was water-saturated). It was important to note that the solubility of pure water in pure DMC is 3 wt% at room temperature while the solubility of pure anhydrous DMC in pure water is 12.7 wt% (Stephenson & Stuart, 1986). In addition, it was recently demonstrated that the carbonyl oxygen of DMC served as the proton acceptor for the hydrogen bonded complex with water (Kar, Ramanathan, Sundararajan, & Viswanathan, 2012). These complexes formation would allow partial solubility of DMC in water. This partial solubility of DMC continuous phase ensured that the exchange was very slow allowing any on-chip precipitation event to occur.

3.6. Solvent diffusion without gelation process

We first looked at the reproducibility of our approach by applying only solvent diffusion to the pectin microdroplets without internal or external gelation in order to evaluate the propensity of DMC to reduce the size of pectin microdroplets and further condensed them in order to eventually produce solid microparticles without the help of a cross-linker. Two immiscible liquids were thus supplied to the flow-focusing device (FFD) by inlet 1 with 1 wt% pectin solution and inlet 2 with anhydrous DMC, respectively, while

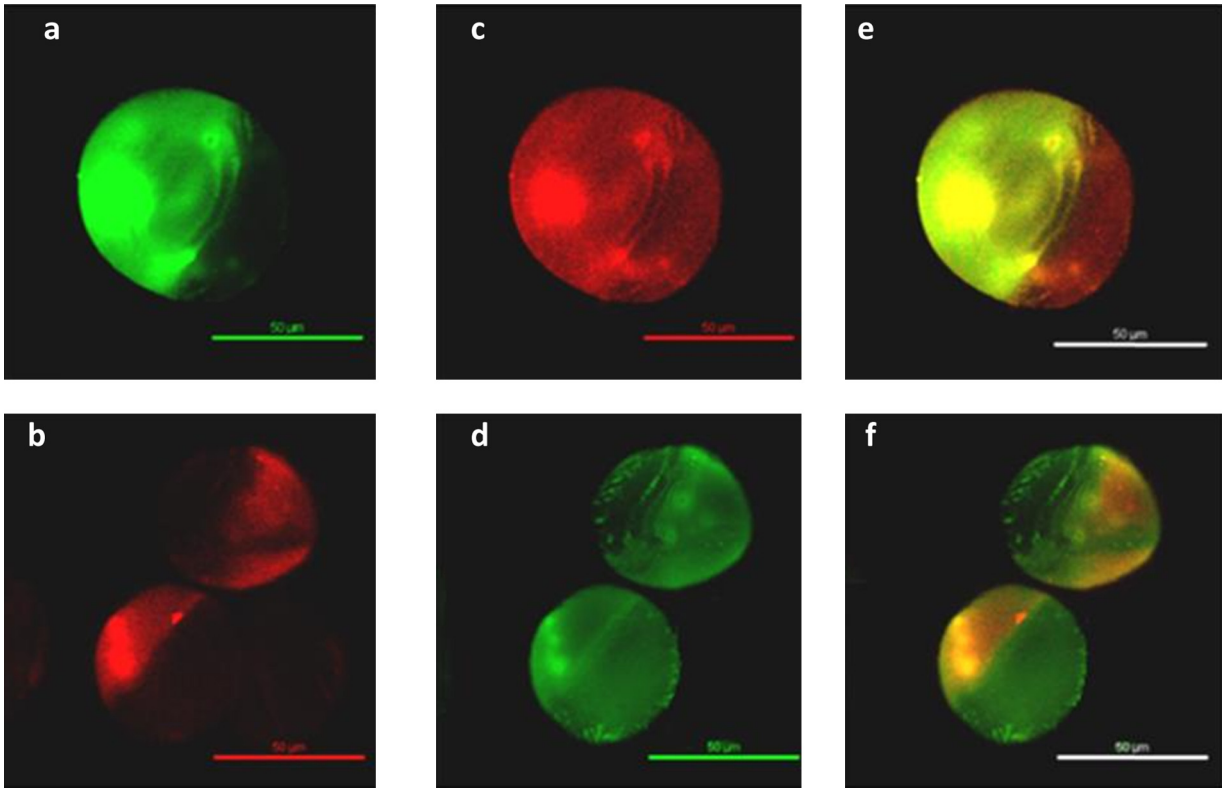

Fig. 5. Confocal scanning laser microscopy images of BSA, free or grafted with dextran, encapsulated in each hemisphere of the pectin–alginate hetero Janus hydrogel microparticles. (a) Alginate_BSA-FITC; (b) Alginate_BSA-RITC-Dextran; (c) Pectin_BSA-RITC-Dextran; (d) Pectin_BSA-FITC; (e, f) Hetero Janus hydrogel microparticles with FITC and RITC-Dextran colour superimposition. Scale bars: 50 µm.

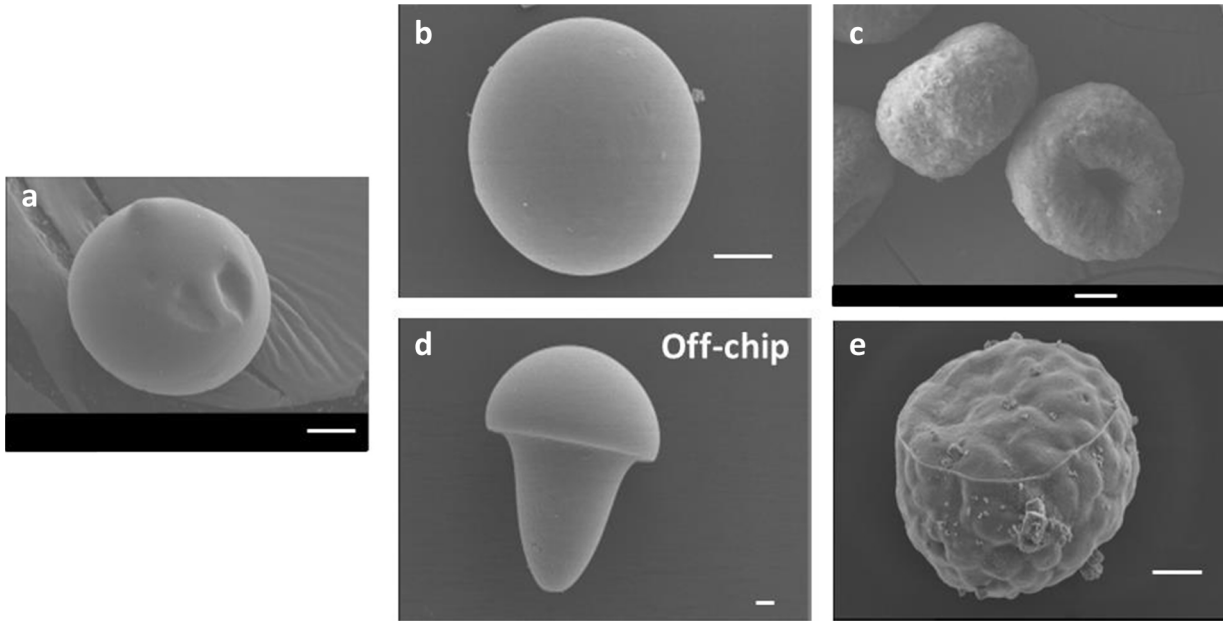

Fig. 6. Scanning electronic microscopy images of pectin hydrogel microparticles obtained by (a) solvent diffusion thanks to anhydrous DMC without cross-linking step, (b) solvent diffusion and external gelation dispersed phase thanks to $CaCl_2$ cross-linking agent, (c) solvent diffusion and internal gelation dispersed phase thanks to $CaCO_3$ cross-linking agent, (d) without solvent diffusion and external gelation, and (e) without solvent diffusion and internal gelation. Scale bars: 10 μm.

water-saturated DMC was supplied by inlet 3 (Fig. 2). By this way, spherical microparticles with smooth surfaces were obtained with an average diameter of 42 μm (Fig. 6a). A three-fold reduction in size was obtained from the initial microdroplets ($D \sim 125$ μm) with a dispersed and continuous phases pressure of, respectively, 600 (inlet 1) and 625 (inlet 2) and 400 (inlet 3) mbar. This size reduction provided strong evidence of significant losses of water to the DMC phase during transport of microdroplets downstream. An estimation of pectin concentration from the volume of the microparticles gave 20.4 wt% (from an initial pectin concentration of 1.1 wt%). The high pectin concentration obtained after solvent diffusion leading to a very condensed phase within microdroplets was confirmed by the unchanged of size of the microparticles observed by phase contrast optical and scanning electron microscopies.

3.7. Solvent diffusion and (external or internal) gelation

A two-step process was adopted in this case with a combination of a solvent diffusion process in order to shrink pectin microdroplets and reduce their size and a gelation process in order to cross-link pectin chains within microdroplets by cation bridging through external or internal gelation (Fig. 2). Two immiscible liquids were thus supplied to the flow-focusing device (FFD) by inlet 1 with 0.5, 1 or 2 wt% pectin solution (or pectin + $CaCO_3$) and inlet 2 with anhydrous DMC, respectively, while $CaCl_2$-saturated DMC (or acetic acid-saturated DMC) was supplied by inlet 3. It was important to note that due to the solubility properties of DMC in water (3 wt%), it was necessary for external gelation to solubilize calcium chloride in DMC at a concentration of 30 wt% giving a final soluble $CaCl_2$ concentration in DMC of 0.9 wt%. For internal gelation process, acetic acid was solubilized in DMC at 5 wt% giving a final acetic acid soluble concentration in DMC of 0.15 wt%.

Hydrogel microparticles formed by solvent diffusion and external gelation through $CaCl_2$ ion bridging displayed either doughnut-like either spherical-like shape depending on initial pectin concentration (Fig. 6b). Deformation of pre-gelled microdroplets was seen by confocal microscopy (data not shown) highlighting both the effect of anisotropic solvent diffusion on the doughnut-like particles formation and the non-equilibrium gel state of microparticles at the end of the on-chip process. The non-equilibrium gel state hypothesis would come from the spherical shape of microparticles obtained when only solvent diffusion proceed and that it was previously demonstrated that the binding of anionic polysaccharides such as pectin to their adapted ion of choice took place on the order of milliseconds to seconds (Goodall & Norton, 1987). The anisotropic shape of microparticles was however not maintained at pectin concentration of 1 and 2 wt%, due presumably to the higher pectin:calcium molar ratio leading to an equilibrium gel state of hydrogel microparticles at the end of the on-chip process.

Hydrogel microparticles formed by solvent diffusion and internal gelation through $CaCO_3$ ion solubilization displayed doughnut-like shape whatever the initial pectin concentration (Fig. 6c). It appeared that the gelation process induced by solubilization of $CaCO_3$ particles after acidification by diffusion of acetic acid from the continuous DMC phase to the aqueous pectin microdroplets would be at the origin of the anisotropic shape of the hydrogel microparticles. Doughnut-like shape would result from the limited diffusion of proton ions during the fast droplet translating in channels from continuous phase that release calcium ions at the periphery of droplets.

3.8. (External or internal) gelation without solvent diffusion process

In this second two-step process, DMC continuous phase was saturated with water in order to prevent solvent diffusion then (external or internal) gelation was applied according to calcium ions bridging. It was therefore demonstrated that the invert process, i.e. (external or internal) gelation preceding the absence of solvent diffusion thanks to water saturated DMC, did not affect the size and shape of pectin hydrogel microparticles (data not shown).

Pectin hydrogel microparticles formed at $C = 1$ wt% after external gelation without solvent diffusion were spherical or slightly elliptical at the end of the on-chip process but were drastically deformed when falled into the $CaCl_2$-DMC interface collecting tube. The resulting anisotropic shape of the microparticles with a

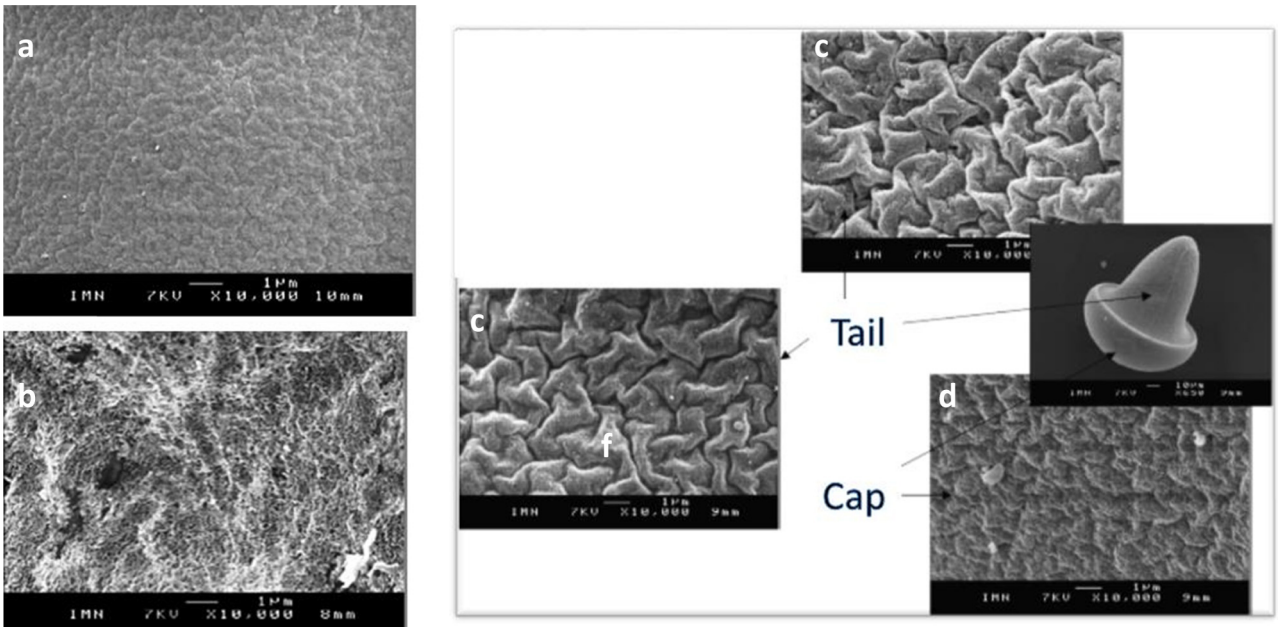

Fig. 7. SEM micrographs of the surface of pectin hydrogel microparticles. (a) Surface of pectin hydrogel microparticles when solvent diffusion applied; (b) surface of pectin hydrogel microparticles without solvent diffusion; (c) tail surface of the mushroom-like morphology microparticles; (d) cap surface of the mushroom-like morphology microparticles. Scale bars: 1 μm.

mushroom-like morphology was clearly visible by optical and electronic microscopies (Fig. 6d). The anisotropic shape obtained in this case was in accordance with previous results, when solvent diffusion occurred (see Section 3.7), where the hydrogel microparticles were in a non-equilibrium state at the end of the on-chip process. The pre-crosslinking reaction of the droplets in the DMC phase saturated with $CaCl_2$ did not make them completely solidified. Thus, when the droplets diffused through the $CaCl_2$–DMC interface, the effect of an impact force led to the formation of a flat bottom of the droplet while the upper half of the droplets retained a spherical shape. More interestingly, the shapes of the hydrogel microparticles were maintained after supercritical drying (Fig. 6d). A similar morphology was previously demonstrated in the case of alginate microgel particles where the authors, by combining microfluidic and external ionic crosslinking, were able to produce mushroom-like, hemi-spherical and red blood cell-like morphologies (Hu et al., 2012). The control of shape was driven by simply varying the gelation conditions (viscosity of the gelation bath, collecting height, interfacial tension) and authors explained that the mushroom-like morphology was due to interplay between the viscous and elastic forces of prolate microdroplets during the subsequent gelation process inside the collecting tubing. Other recent paper reported the production of macroscopic mushroom-like structures made of alginate (Mele et al., 2013). In our study, the interfacial properties of the $CaCl_2$–DMC interface could be the driving force of the deformation of the pre-gelled microdroplets. The pre-gelled microdroplets will become oblate due to the interplay between interfacial tension and gravity during the falling process. A protrusion from the oblate shape microdroplets would allow a tail to gradually grow up, owing to the mushroom-like morphology to be formed when pre-gelled microdroplets crossed the $CaCl_2$–DMC interface. However, Rondeau and Cooper-White (2008) noted that the interfacial tension for alginate was very close to the value for water and DMC ($\gamma_{water/DMC} = 5.31$ vs. $\gamma_{alginate/DMC} = 4.95$ mN/m) and did not depend on the alginate concentration. This finding may question about the driving force of microdroplets deformation in our pectin hydrogel microparticles when they crossed the $CaCl_2$–DMC interface. The most probable hypothesis would be that our pectin sample at the concentrations used (0.5–2 wt%) and/or our DMC continuous phase, as it was $CaCl_2$ saturated, would lead to a much more greater interfacial tension value, allowing a deformation of the pre-gelled pectin microdroplets. This hypothesis would be reinforced by the fact that hydrogel microparticles formed by the same process but with an additional solvent diffusion step were never deformed due to their higher pectin concentrations, the condensed state of the particles being unaffected off-chip by the $CaCl_2$–DMC interface.

Pectin hydrogel microparticles formed by internal gelation through $CaCO_3$ ion solubilization and bridging without solvent diffusion displayed spherical and doughnut-like shapes at initial pectin concentration of 0.5 and 1 wt% while oblate elliptical shape was obtained at $C = 2$ wt% (Fig. 6e). The transition morphology observed during this process was very similar to what was observed in the process where solvent diffusion occurred, the main difference being observed for pectin hydrogel microparticles formed at $C = 2$ wt%. While a doughnut-like morphology was observed when solvent diffusion occurred, an oblate elliptical shape with a raspberry-like morphology was visible when solvent diffusion did not occur.

The doughnut-like shape of hydrogel microparticles obtained by internal or external gelation and solvent diffusion could be rationalized considering the Peclet number ($P_e = (R^2/\tau_d D)$, with R the radius of the initial microdroplet ($R = ½D_0$), D the pectin diffusion coefficient and τ_d the time required for a microdroplet to dry) experienced by the microdroplets (Marquis, Davy, Fang, & Renard, 2013). Fang et al. identified for silica particles two zones corresponding to two different particle shapes using DMC as continuous phase: either doughnut-like or bowl-like shape for $P_e \gg 1$ (Fang et al., 2012). In addition, the morphological transition from bowl-like to doughnut-like shape occurred for $D_0/h = 0.8$, with D_0 the initial droplet size and h the serpentine microchannel height. In our study, and according to the rationalization of shape changes with DMC continuous phase, our respective D_0/h and P_e number values determined for internal and external gelation fell in the doughnut-like regime identified by Fang et al. (Marquis et al., 2013).

3.9. Surface microstructure of pectin hydrogel microparticles

The microstructure of the surface of pectin hydrogel microparticles probed by SEM was useful in an attempt to correlate microfluidic diffusion induced self-assembly and surface porosity. The solvent diffusion process coupled to gelation (internal or external) or to the absence of gelation had no drastic effects on the surface microstructure of pectin hydrogel microparticles (Fig. 7). The rather smooth surfaces were uniformly covered due to the condensation and thereafter pectin chains merging induced by water uptake from DMC continuous phase (Fig. 7a). In addition, the mode of gelation and the pectin concentration had no impact on the surface of microparticles contrary to what was observed on their shape. Without solvent diffusion, the morphological transitions previously observed on microparticles were accompanied by drastic changes on their surfaces (Fig. 7b). In the case of internal gelation, surfaces were irregular with an inhomogeneous pectin distribution. An interconnected pectin chains network was clearly visible on the surface of the microparticles with a pore size distribution ranging from 100 up to 600 nm. The increase of pectin concentration had however a "smoothing" effect on the surface of the microparticles with a better homogeneity and no voids (data not shown). Finally, in the particular case of the formation of mushroom-type morphology (i.e. external gelation without solvent diffusion), the tail surface of the "mushroom" displayed rather loosely interconnected anisotropic "domains" (with a star-like shape) with some interspersed voids (Fig. 7c). The cap surface was made of tightly interspersed more or less spherical "domains" giving rise to an undulated surface (Fig. 7d). The surface topology of the mushroom-like morphology microparticles would reinforce the hypothesis of the non-uniformity of pectin crosslinking during the gelation process leading to the deformation of the pre-gelled microdroplets at the $CaCl_2$–DMC interface. Moreover, it was established that after crossing the DMC – $CaCl_2$ liquid–liquid interface during their collect, the mushroom-like morphology microparticles did not migrate in the calcium or DMC phase but stayed at the interface (data not shown). The interfacial positioning of the microparticles was also noticed after manual shaking or after a centrifugation step. This unexpected result questions about the relationship that could exist between the surface structure and the liquid–liquid interface stabilizer property of these microparticles.

4. Conclusion

This study demonstrated the use of microfluidics to generate Janus microbeads and microparticles with complex shapes from polysaccharides. The design of the microdevice for Janus microparticles production, coupled with optimization of the chemical route of biopolymer gelation, allowed the production of homo and hetero Janus hydrogel microparticles from pectin–pectin and pectin–alginate with a well-defined interface, particularly in the case of hetero Janus microparticles, thanks to specific interactions between the two polysaccharides. We also demonstrated the selective degradation by enzymatic hydrolysis as well as BSA encapsulation in each hemisphere of the biopolymer-based hydrogel microparticles. Future investigations will focus on the release of compounds embedded in biopolymer networks and their control by fine-tuning of the network structure and enzymatic hydrolysis conditions.

We also demonstrated the generation of pectin hydrogel microparticles of complex shapes by combining the phenomenon of gelation and water diffusion induced self-assembly in microfluidic channels (on-chip) or by the deformation of the pre-gelled droplets outside the channels (off-chip) at a fluid–fluid interface. We proved that by tuning the mode of pectin cross-linking ($CaCl_2$ vs. $CaCO_3$) and the degree of shrinking (water content in the organic continuous phase) we can control the shape of the final particle. Sphere, doughnut-like, oblate ellipsoid or mushroom-like morphologies were thus produced and demonstrated the ability of the control of formation of anisotropic biopolymer-based hydrogel microparticles using microfluidics. In perspective, the swelling behaviour of these microparticles will be investigated as a function of pH and in the particular case of mushroom-type morphology, the ability to stabilize liquid–liquid interfaces will be explored.

The microfluidics process used in this study will therefore provide new opportunities for the release of active substances in a controlled environment and could find applications in food, medicine and cosmetics. Our approach could also be extended to hydrogel microparticles formation from other anionic biopolymers, providing new opportunities to produce biomimetic microgels with various anisotropic dimensions for the applications in drug delivery, optical devices and in advanced materials formation.

Acknowledgments

We would like to acknowledge the Biopolymers Interactions Structural Biology platform (INRA, Nantes) and in particular, B. Bouchet, for use of the confocal scanning laser microscope and its fruitful guidance during observations. We are grateful to E. Bonnin (INRA, Nantes) for her expertise in experimental enzymatic hydrolysis and N. Stephan for MEB facilities and expertise at IMN (Nantes, France).

References

Bellich, B., Borgogna, M., Cok, M., & Cesaro, A. (2011). Release properties of hydrogels: Water evaporation from alginate gel beads. *Food Biophysics*, *6*(2), 259–266.
Berkland, C., Kim, K. K., & Pack, D. W. (2001). Fabrication of PLG microspheres with precisely controlled and monodisperse size distributions. *Journal of Controlled Release*, *73*(1), 59–74.
Biggs, A. R., ElKholi, M. M., ElNeshawy, S., & Nickerson, R. (1997). Effects of calcium salts on growth, polygalacturonase activity, and infection of peach fruit by Monilinia fructicola. *Plant Disease*, *81*(4), 399–403.
Boeker, A., He, J., Emrick, T., & Russell, T. P. (2007). Self-assembly of nanoparticles at interfaces. *Soft Matter*, *3*(10), 1231–1248.
Bonnin, E., Le Goff, A., Korner, R., Vigouroux, J., Roepstorff, P., & Thibault, J. F. (2002). Hydrolysis of pectins with different degrees and patterns of methylation by the endopolygalacturonase of Fusarium moniliforme. *Biochimica et Biophysica Acta: Protein Structure and Molecular Enzymology*, *1596*(1), 83–94.
Carturan, G., Dal Toso, R., Boninsegna, S., & Dal Monte, R. (2004). Encapsulation of functional cells by sol-gel silica: Actual progress and perspectives for cell therapy. *Journal of Materials Chemistry*, *14*(14), 2087–2098.
Champion, J. A., Katare, Y. K., & Mitragotri, S. (2007). Particle shape: A new design parameter for micro- and nanoscale drug delivery carriers. *Journal of Controlled Release*, *121*(1–2), 3–9.
Champion, J. A., & Mitragotri, S. (2006). Role of target geometry in phagocytosis. *Proceedings of the National Academy of Sciences of the United States of America*, *103*(13), 4930–4934.
Charnay, C., Lee, A., Man, S. Q., Moran, C. E., Radloff, C., Bradley, R. K., & Halas, N. J. (2003). Reduced symmetry metallodielectric nanoparticles: Chemical synthesis and plasmonic properties. *Journal of Physical Chemistry B*, *107*(30), 7327–7333.
Chawla, K., Yu, T. B., Liao, S. W., & Guan, Z. B. (2011). Biodegradable and biocompatible synthetic saccharide-peptide hydrogels for three-dimensional stem cell culture. *Biomacromolecules*, *12*(3), 560–567.
Cho, I., & Lee, K. W. (1985). Morphology of latex-particules formed by poly(methyl methacrylate)-seeded emulsion polymerization of styrene. *Journal of Applied Polymer Science*, *30*(5), 1903–1926.
Cho, Y.-S., Yi, G.-R., Kim, S.-H., Jeon, S.-J., Elsesser, M. T., Yu, H. K., Yang, S.-M., & Pine, D. J. (2007). Particles with coordinated patches or windows from oil-in-water emulsions. *Chemistry of Materials*, *19*(13), 3183–3193.
Cui, J.-Q., & Kretzschmar, I. (2006). Surface-anisotropic polystyrene spheres by electroless deposition. *Langmuir*, *22*(20), 8281–8284.
Dai, C. Y., Wang, B. C., & Zhao, H. W. (2005). Microencapsulation peptide and protein drugs delivery system. *Colloids and Surfaces B: Biointerfaces*, *41*(2–3), 117–120.
Dang, T. D., & Joo, S. W. (2013). Preparation of tadpole-shaped calcium alginate microparticles with sphericity control. *Colloids and Surfaces B: Biointerfaces*, *102*, 766–771.
De Geest, B. G., Urbanski, J. P., Thorsen, T., Demeester, J., & De Smedt, S. C. (2005). Synthesis of monodisperse biodegradable microgels in microfluidic devices. *Langmuir*, *21*(23), 10275–10279.
Dendukuri, D., Tsoi, K., Hatton, T. A., & Doyle, P. S. (2005). Controlled synthesis of nonspherical microparticles using microfluidics. *Langmuir*, *21*(6), 2113–2116.

Du, J., & O'Reilly, R. K. (2011). Anisotropic particles with patchy, multicompartment and Janus architectures: Preparation and application. *Chemical Society Reviews*, *40*(5), 2402–2416.

Fang, A., Gaillard, C., & Douliez, J.-P. (2011). Template-free formation of monodisperse doughnut-shaped silica microparticles by droplet-based microfluidics. *Chemistry of Materials*, *23*(21), 4660–4662.

Fang, A., Gosse, C., Gaillard, C., Zhao, X., & Davy, J. (2012). Tuning silica particle shape at fluid interfaces. *Lab on a Chip*, *12*(23), 4960–4963.

Glotzer, S. C., & Solomon, M. J. (2007). Anisotropy of building blocks and their assembly into complex structures. *Nature Materials*, *6*(8), 557–562.

Gohil, R. M. (2010). Synergistic blends of natural polymers, pectin and sodium alginate. *Journal of Applied Polymer Science*, *120*(4), 2324–2336.

Goodall, D. M., & Norton, I. T. (1987). Polysaccharide conformations and kinetics. *Accounts of Chemical Research*, *20*(2), 59–65.

Haynes, C. L., & Van Duyne, R. P. (2001). Nanosphere lithography: A versatile nanofabrication tool for studies of size-dependent nanoparticle optics. *Journal of Physical Chemistry B*, *105*(24), 5599–5611.

Howse, J. R., Jones, R. A. L., Ryan, A. J., Gough, T., Vafabakhsh, R., & Golestanian, R. (2007). Self-motile colloidal particles: From directed propulsion to random walk. *Physical Review Letters*, *99*(4), 048102.

Hu, Y., Wang, Q., Wang, J., Zhu, J., Wang, H., & Yang, Y. (2012). Shape controllable microgel particles prepared by microfluidic combining external ionic crosslinking. *Biomicrofluidics*, *6*(2), 026502.

Jeong, W., Kim, J., Kim, S., Lee, S., Mensing, G., & Beebe, D. J. (2004). Hydrodynamic microfabrication via "on the fly" photopolymerization of microscale fibers and tubes. *Lab on a Chip*, *4*(6), 576–580.

Jiang, S., Chen, Q., Tripathy, M., Luijten, E., Schweizer, K. S., & Granick, S. (2010). Janus particle synthesis and assembly. *Advanced Materials*, *22*(10), 1060–1071.

Kar, B. P., Ramanathan, N., Sundararajan, K., & Viswanathan, K. S. (2012). Conformations of dimethyl carbonate and its complexes with water: A matrix isolation infrared and ab initio study. *Journal of Molecular Structure*, *1024*, 84–93.

Lahann, J. (2011). Recent progress in nano-biotechnology: Compartmentalized micro- and nanoparticles via electrohydrodynamic co-jetting. *Small*, *7*(9), 1149–1156.

Lewis, C. L., Lin, Y., Yang, C., Manocchi, A. K., Yuet, K. P., Doyle, P. S., & Yi, H. (2010). Microfluidic fabrication of hydrogel microparticles containing functionalized viral nanotemplates. *Langmuir*, *26*(16), 13436–13441.

Liu, K., Ding, H. J., Liu, J., Chen, Y., & Zhao, X. Z. (2006). Shape-controlled production of biodegradable calcium alginate gel microparticles using a novel microfluidic device. *Langmuir*, *22*(22), 9453–9457.

Liu, X. D., Bao, D. C., Xue, W. M., Xiong, Y., Yu, W. T., Yu, X. J., Ma, X. J., & Yuan, Q. (2003). Preparation of uniform calcium alginate gel beads by membrane emulsification coupled with internal gelation. *Journal of Applied Polymer Science*, *87*(5), 848–852.

Manoharan, V. N., Elsesser, M. T., & Pine, D. J. (2003). Dense packing and symmetry in small clusters of microspheres. *Science*, *301*(5632), 483–487.

Marquis, M., Davy, J., Fang, A., & Renard, D. (2013). Microfluidics assisted diffusion self-assembly: towards a control of shape and size of pectin hydrogel microparticles. *Biomacromolecules*, under revision.

Marquis, M., Renard, D., & Cathala, B. (2012). Microfluidic generation and selective degradation of biopolymer-based Janus microbeads. *Biomacromolecules*, *13*(4), 1197–1203.

Mele, E., Fragouli, D., Ruffilli, R., De Gregorio, G. L., Cingolani, R., & Athanassiou, A. (2013). Complex architectures formed by alginate drops floating on liquid surfaces. *Soft Matter*, *9*(27), 6338–6343.

Nie, Z. H., Li, W., Seo, M., Xu, S. Q., & Kumacheva, E. (2006). Janus and ternary particles generated by microfluidic synthesis: Design, synthesis, and self-assembly. *Journal of the American Chemical Society*, *128*, 9408–9412.

Nie, Z. H., Xu, S. Q., Seo, M., Lewis, P. C., & Kumacheva, E. (2005). Polymer particles with various shapes and morphologies produced in continuous microfluidic reactors. *Journal of the American Chemical Society*, *127*(22), 8058–8063.

Nisisako, T., & Hatsuzawa, T. (2009). A microfluidic cross-flowing emulsion generator for producing biphasic droplets and anisotropically shaped polymer particles. *Microfluidics and Nanofluidics*, *9*(2–3), 427–437.

Nisisako, T., Torii, T., Takahashi, T., & Takizawa, Y. (2006). Synthesis of monodisperse bicolored janus particles with electrical anisotropy using a microfluidic co-flow system. *Advanced Materials*, *18*(9), 1152–1156.

Ogushi, Y., Sakai, S., & Kawakami, K. (2007). Synthesis of enzymatically-gellable carboxymethylcellulose for biomedical applications. *Journal of Bioscience and Bioengineering*, *104*(1), 30–33.

Ouwerx, C., Velings, N., Mestdagh, M. M., & Axelos, M. A. V. (1998). Physico-chemical properties and rheology of alginate gel beads formed with various divalent cations. *Polymer Gels and Networks*, *6*(5), 393–408.

Peppas, N. A., Hilt, J. Z., Khademhosseini, A., & Langer, R. (2006). Hydrogels in biology and medicine: From molecular principles to bionanotechnology. *Advanced Materials*, *18*(11), 1345–1360.

Perro, A., Reculusa, S., Ravaine, S., Bourgeat-Lami, E. B., & Duguet, E. (2005). Design and synthesis of Janus micro- and nanoparticles. *Journal of Materials Chemistry*, *15*(35–36), 3745–3760.

Petit, L., Manaud, J. P., Mingotaud, C., Ravaine, S., & Duguet, E. (2001). Sub-micrometer silica spheres dissym-metrically decorated with gold nanoclusters. *Materials Letters*, *51*(6), 478–484.

Poortinga, A. T. (2008). Microcapsules from self-assembled colloidal particles using aqueous phase-separated polymer solutions. *Langmuir*, *24*(5), 1644–1647.

Rahman, M. M., Montagne, F., Fessi, H., & Elaissari, A. (2010). Anisotropic magnetic microparticles from ferrofluid emulsion. *Soft Matter*, *7*(4), 1483–1490.

Ralet, M. C., Bonnin, E., & Thibault, J. F. (2001). Chromatographic study of highly methoxylated lime pectins deesterified by different pectin methyl-esterases. *Journal of Chromatography B*, *753*(1), 157–166.

Robitzer, M., David, L., Rochas, C., Di Renzo, F., & Quignard, F. (2008). Supercritically-dried alginate aerogels retain the fibrillar structure of the hydrogels. *Macromolecular Symposia*, *273*, 80–84.

Rondeau, E., & Cooper-White, J. J. (2008). Biopolymer microparticle and nanoparticle formation within a microfluidic device. *Langmuir*, *24*(13), 6937–6945.

Sarrazin, F., Bonometti, T., Prat, L., Gourdon, C., & Magnaudet, J. (2008). Hydrodynamic structures of droplets engineered in rectangular micro-channels. *Microfluidics and Nanofluidics*, *5*(1), 131–137.

Seo, M., Nie, Z. H., Xu, S. Q., Lewis, P. C., & Kumacheva, E. (2005). Microfluidics: From dynamic lattices to periodic arrays of polymer disks. *Langmuir*, *21*(11), 4773–4775.

Serra, C. A., & Chang, Z. Q. (2008). Microfluidic-assisted synthesis of polymer particles. *Chemical Engineering & Technology*, *31*(8), 1099–1115.

Shepherd, R. F., Conrad, J. C., Rhodes, S. K., Link, D. R., Marquez, M., Weitz, D. A., & Lewis, J. A. (2006). Microfluidic assembly of homogeneous and janus colloid-filled hydrogel granules. *Langmuir*, *22*(21), 8618–8622.

Siracusa, V., Rocculi, P., Romani, S., & Dalla Rosa, M. (2008). Biodegradable polymers for food packaging: A review. *Trends in Food Science & Technology*, *19*(12), 634–643.

Snyder, C. E., Yake, A. M., Feick, J. D., & Velegol, D. (2005). Nanoseale functionalization and site-specific assembly of colloids by particle lithography. *Langmuir*, *21*(11), 4813–4815.

Stahler, K., Selb, J., & Candau, F. (1999). A study of multicompartment polymeric micelles. *Materials Science & Engineering C: Biomimetic and Supramolecular Systems*, *10*(1–2), 171–178.

Stephenson, R., & Stuart, J. (1986). Mutual binary solubilities-water alcohols and water esters. *Journal of Chemical and Engineering Data*, *31*(1), 56–70.

Sugiura, S., Oda, T., Izumida, Y., Aoyagi, Y., Satake, M., Ochiai, A., Ohkohchi, N., & Nakajima, M. (2005). Size control of calcium alginate beads containing living cells using micro-nozzle array. *Biomaterials*, *26*(16), 3327–3331.

Thiang Yian, W., Preston, L. A., & Schiller, N. L. (2000). Alginate lyase: Review of major sources and enzyme characteristics, structure-function analysis, biological roles, and applications. *Annual Review of Microbiology*, *54*(54), 289–340.

Tung, K. Y., Li, C. C., & Yang, J. T. (2009). Mixing and hydrodynamic analysis of a droplet in a planar serpentine micromixer. *Microfluidics and Nanofluidics*, *7*(4), 545–557.

Ulery, B. D., Nair, L. S., & Laurencin, C. T. (2011). Biomedical Applications of Biodegradable Polymers. *Journal of Polymer Science Part B: Polymer Physics*, *49*(12), 832–864.

Um, E., Lee, D. S., Pyo, H. B., & Park, J. K. (2008). Continuous generation of hydrogel beads and encapsulation of biological materials using a microfluidic droplet-merging channel. *Microfluidics and Nanofluidics*, *5*(4), 541–549.

Walther, A., Hoffmann, M., & Mueller, A. H. E. (2008). Emulsion polymerization using Janus particles as stabilizers. *Angewandte Chemie-International Edition*, *47*(4), 711–714.

Xu, S. Q., Nie, Z. H., Seo, M., Lewis, P., Kumacheva, E., Stone, H. A., Garstecki, P., Weibel, D. B., Gitlin, I., & Whitesides, G. M. (2005). Generation of monodisperse particles by using microfluidics: Control over size, shape, and composition. *Angewandte Chemie-International Edition*, *44*(5), 724–728.

Yamada, M., Sugaya, S., Naganuma, Y., & Seki, M. (2012). Microfluidic synthesis of chemically and physically anisotropic hydrogel microfibers for guided cell growth and networking. *Soft Matter*, *8*(11), 3122–3130.

Yang, C.-H., Huang, K.-S., Wang, C.-Y., Hsu, Y.-Y., Chang, F.-R., & Lin, Y.-S. (2012). Microfluidic-assisted synthesis of hemispherical and discoidal chitosan microparticles at an oil/water interface. *Electrophoresis*, *33*(21), 3173–3180.

Yin, Y. D., & Xia, Y. N. (2001). Self-assembly of monodispersed spherical colloids into complex aggregates with well-defined sizes, shapes, and structures. *Advanced Materials*, *13*(4), 267–271.

Yoshida, M., & Lahann, J. (2008). Smart nanomaterials. *Acs Nano*, *2*(6), 1101–1107.

Zhang, H., Nunes, J. K., Gratton, S. E. A., Herlihy, K. P., Pohlhaus, P. D., & DeSimone, J. M. (2009). Fabrication of multiphasic and regio-specifically functionalized PRINT (R) particles of controlled size and shape. *New Journal of Physics*, *11*(11), 075018.

Zhang, H., Tumarkin, E., Sullan, R. M. A., Walker, G. C., & Kumacheva, E. (2007). Exploring microfluidic routes to microgels of biological polymers. *Macromolecular Rapid Communications*, *28*(5), 527–538.

Zhang, H. W., Betz, A., Qadeer, A., Attinger, D., & Chen, W. L. (2010). Microfluidic formation of monodispersed spherical microgels composed of triple-network crosslinking. *Journal of Applied Polymer Science*, *121*(5), 3093–3100.

Zhang, X. Z., Lewis, P. J., & Chu, C. C. (2005). Fabrication and characterization of a smart drug delivery system: Microsphere in hydrogel. *Biomaterials*, *26*(16), 3299–3309.

Zhao, L. B., Pan, L., Zhang, K., Guo, S. S., Liu, W., Wang, Y., Chen, Y., Zhao, X. Z., & Chan, H. L. W. (2009). Generation of Janus alginate hydrogel particles with magnetic anisotropy for cell encapsulation. *Lab on a Chip*, *9*(20), 2981–2986.

Zheng, B., Tice, J. D., & Ismagilov, R. F. (2004). Formation of droplets of in microfluidic channels alternating composition and applications to indexing of concentrations in droplet-based assays. *Analytical Chemistry*, *76*(17), 4977–4982.

Zykwinska, A., Gaillard, C., Boiffard, M.-H., Thibault, J.-F., & Bonnin, E. (2009). "Green labelled" pectins with gelling and emulsifying properties can be extracted by enzymatic way from unexploited sources. *Food Hydrocolloids*, *23*(8), 2468–2477.